



**HAL**  
open science

# Simplified Modelling of the Infrared Heating Involving the Air Convection Effect before the Injection Stretch Blowing Moulding of PET Preform

Yun Mei Luo, Luc Chevalier, Françoise Utheza, Xavier Nicolas

► **To cite this version:**

Yun Mei Luo, Luc Chevalier, Françoise Utheza, Xavier Nicolas. Simplified Modelling of the Infrared Heating Involving the Air Convection Effect before the Injection Stretch Blowing Moulding of PET Preform. Material Forming ESAFORM 2014, May 2014, Espoo, Finland. pp.844-851, 10.4028/www.scientific.net/KEM.611-612.844 . hal-01077292

**HAL Id: hal-01077292**

**<https://hal.science/hal-01077292v1>**

Submitted on 24 Oct 2014

**HAL** is a multi-disciplinary open access archive for the deposit and dissemination of scientific research documents, whether they are published or not. The documents may come from teaching and research institutions in France or abroad, or from public or private research centers.

L'archive ouverte pluridisciplinaire **HAL**, est destinée au dépôt et à la diffusion de documents scientifiques de niveau recherche, publiés ou non, émanant des établissements d'enseignement et de recherche français ou étrangers, des laboratoires publics ou privés.

# Simplified Modelling of the Infrared Heating Involving the Air Convection Effect before the Injection Stretch Blowing Moulding of PET Preform

Yun Mei Luo<sup>a\*</sup>, Luc Chevalier<sup>b</sup>, Françoise Utheza<sup>c</sup> and Xavier Nicolas<sup>d</sup>

Université Paris-Est, Laboratoire Modélisation et Simulation Multi Echelle, MSME UMR 8208  
CNRS, 5 bd Descartes, 77454 Marne-la-Vallée, France

<sup>a</sup>yunmei.luo@univ-paris-est.fr, <sup>b</sup>luc.chevalier@univ-paris-est.fr, <sup>c</sup>francoise.utheza@univ-paris-est.fr, <sup>d</sup>xavier.nicolas@univ-paris-est.fr

**Keywords:** Numerical simulation, Infrared heating, Air convection effect, PET preform

**Abstract:** Initial heating conditions and temperature effects (heat transfer with air and mould, self-heating, conduction) have important influence during the ISBM process of PET preforms. The numerical simulation of infrared (IR) heating taking into account the air convection around a PET preform is very time-consuming even for 2D modelling. This work proposes a simplified approach of the coupled heat transfers (conduction, convection and radiation) in the ISBM process based on the results of a complete IR heating simulation of PET sheet using ANSYS/Fluent. First, the simplified approach is validated by comparing the experimental temperature distribution of a PET sheet obtained from an IR camera with the numerical results of the simplified simulation. Second, we focus on the more complex problem of the rotating PET preform heated by IR lamps. This problem cannot be modeled in 2D and the complete 3D approach is out of calculation possibilities actually. In our approach, the IR heating flux coming from IR lamps is calculated using radiative laws adapted to the test geometry. Finally, the simplified approach used on the 2D plane sheet case to model the air convection is applied to the heat transfer between the cylindrical preform and ambient air using a simple model in Comsol where only the preform is meshed. In this case, the effect of the rotation of the preform is taken into account in the radiation flux by a periodic time function. The convection effect is modeled through the thermal boundary conditions at the preform surface using the heat transfer coefficients exported from the simulations of the IR heating of a PET sheet with ANSYS/Fluent. The temperature distribution on the outer surface of the preform is compared to the thermal imaging for validation.

## Introduction

The effects of temperature and the initial heating conditions have a fundamental importance during the ISBM process of PET preforms. The mechanical properties of PET are related to the microstructural morphology of the material and strongly depend on the process temperature as well as on the strain rates. There is a great industrial interest to be able to predict the temperature distribution at the beginning and during the ISBM process: it is a scientific problem that has been addressed by numerous authors during the 15 last years. Many experimental researches [1-3] and numerical ones [4-6], especially during the last decade, have been carried out to develop competitive processes and to optimize the IR radiation step. Regarding the numerical approach, the works focus on the IR heating modelling and do not consider the natural convection of air in the boundary conditions. Regarding the experimental approach, the researches have no means to accurately measure the internal surface temperature. However, the provided data of the external surface temperature are very helpful to validate the simulation of the IR heating.

Our previous papers [7,8] were a first contribution on the thermal aspects of the ISBM process, in which the procedure for the identification of the thermal properties is managed on PET sheets from infrared (IR) heating tests. The identified parameters were compared to classical values of the literature and the identification of the heat conductivity  $k$ , appeared to be too small (0.1 VS 0.25

$W/m.K$ ). The first section of this work aims at improving the experimental procedure to correct the conductivity value.

Using only radiative flux and constant convection coefficients as boundary conditions of the IR heating of a rotating preform, it is also shown in [8] that the simulation fails to represent accurately the temperature distribution on the height of the preform since the natural convection of air is not taken into account. Thus in the second section of this work, we study the natural convection using the numerical simulation software Ansys/Fluent. The 2D numerical simulation of the coupled heat transfers (conduction, convection and radiation) for the PET sheet is managed. The simulation is very time-consuming even for 2D modelling.

A simplified model of the convective and radiative heat transfers is therefore proposed and solved into Comsol to facilitate the simulation. A non constant convective heat transfer coefficient is exported from the Ansys/Fluent simulation and then, is set as the boundary conditions in the 3D calculation with Comsol. Furthermore, the modelling of the IR heating is obtained by simply introducing an appropriate heat source term into the PET sheet. Thanks to this simplified model for convection and radiation, the 3D numerical simulation of the heat equation is very little time consuming into Comsol. The surface temperature distribution of the PET sheets by the thermal imaging is compared to the numerical results. It is shown that the simplified numerical approach upgrades the accuracy of the simulation of the temperature distribution on the surface of the PET sheet.

In the fourth and last section, the IR heating flux coming from IR lamps is studied for the PET preform, using radiative laws adapted to the geometry of the preform. A numerical simulation of the preform heating, taking into account the rotation of the preform in front of the lamps, is performed involving the simplified procedure for convection and radiation. The temperature distribution is compared to the thermal imaging for validation.

## Identification of the thermal properties of the PET sheets

In a previous paper [7], the authors presented the experimental procedure to identify the thermal parameters of the PET using an IR heating apparatus developed in MSME laboratory. They found that the heat conductivity  $k$  was small comparing with the reference. In this work, we use the FLIR B250 infrared camera with the wavelength range  $7.5 - 13 \mu m$  to evaluate the surface temperature distribution. The PET sheet (Arnite D00301 from DSM industries) with the surface dimensions  $125 mm \times 125 mm$  and  $3 mm$  thickness is used for the experiment.

We can fix the thermocouple by a scotch tape on the center point of the rear face. However, for the center point of the front face, in order to measure accurately the temperature on this point without being influenced by the radiation from the lamps, three different modes of setting the thermocouples are presented and tested:

- Thermocouple on the front face fixed by a Scotch tape;
- Thermocouple on the front face fixed by paste plus a scotch tape outside;
- Thermocouple in a hole of  $0.5 mm$  depth from the front face with paste outside.

At steady state, the difference of temperature measured by the thermocouples fixed with the scotch tape and the one fixed by the paste with scotch tape is only  $1^\circ C$ . These two modes of setting the thermocouples overestimate the temperature because the thermocouples receive some radiation from the IR lamps. In order to avoid this problem, one proposes to measure the temperature by the third mode: a hole of  $0.5 mm$  depth with the paste outside to fix the thermocouple. With this fixation, at steady state, the difference of temperature between the rear and front face is about  $6^\circ C$ .

The simulation is limited to a 1D model (depending on thickness) for the identification [7,8]. The temperatures measured by the thermocouples are used to manage the identification. The heat transfer equation in the 1D case with the radiative source term can be written in the following way:

$$\rho C_p (T) \dot{T} - k \frac{\partial^2 T}{\partial z^2} = -div(\vec{q}_r) \quad (1)$$

where:  $\rho$  is the specific mass,  $C_p$  is the specific heat capacity,  $k$  is the material conductivity and  $\vec{q}_r$  is the internal radiative heat flux which is taken also as one dimensional and is managed by the Beer–Lambert law:

$$\vec{q}_r = \phi_{\lambda 0} e^{-k_{\lambda} z} \vec{z} \quad (2)$$

where:  $\phi_{\lambda 0}$  is the incident radiation,  $k_{\lambda}$  is the spectral absorption coefficient of PET and  $z$  represent the path between the front PET surface and the current position.

The boundary conditions are given in the following way:

$$k \vec{\nabla} T \cdot \vec{z} = h_f (T - T_{\infty}) \quad \text{on the face in front of the lamps;} \quad (3a)$$

$$-k \vec{\nabla} T \cdot \vec{z} = h_r (T - T_{\infty}) \quad \text{on the rear face.} \quad (3b)$$

where  $h_f$  and  $h_r$  are the total (convective and radiative emission) heat transfer coefficient on the face in front of the lamps and the one on the rear face.  $T_{\infty}$  is the surrounding bulk temperature (20°C).

The specific mass  $\rho$  and the heat capacity  $C_p$  are considered together as a one parameter  $\rho C_p$  which is a function of the temperature. According to the values referenced in [4], it appears that  $\rho$  is almost independent of the temperature but  $C_p$  increases while the temperature increases. We propose the following function to represent the evolution of the parameter  $\rho C_p$ :

$$\rho C_p = \Delta \rho C_p \arctan(\alpha(T - T_g)) + \rho C_{p1} \quad (4)$$

where  $\Delta \rho C_p$  is a constant related to the amplitude of the increase of the  $\rho C_p$  value when passing from the glassy state to the rubber state,  $T_g$  is the more or less glass transition temperature,  $\rho C_{p1}$  is a value corresponding to the glassy state of the material and  $\alpha$  is a factor that fits the roughness of the jump of the curve.

The Monte Carlo method is used to identify the parameters that best fit the experimental results. The thermal properties are referenced in table 1. The total heat transfer coefficients  $h_f$  and  $h_r$ , the absorption coefficient  $k_{\lambda}$  and the conductivity parameter  $k$  have the same order of magnitude than the one seen in literature (0.25 VS 0.26 W/m.K).

**Table 1.** The value of thermal properties

Parameter	$\rho C_p$ (J/m <sup>3</sup> .K)				$k$ (W/m.K)	$h$ (W/m <sup>2</sup> .K)		$k_{\lambda}$ (/m)
	$\rho C_{p1}$	$T_g$	$\Delta \rho C_p$	$\alpha$		$h_f$	$h_r$	
Value	1.68 10 <sup>5</sup>	87	2.3 10 <sup>6</sup>	0.1	0.26	10	11	3.10 <sup>4</sup>

Figure 1 shows the experimental temperature evolution on the surface in front of the lamps  $T_f$  and the one on the rear face  $T_r$  (lines). With the identified parameters, the curves obtained have a good representation of the experimental results (dots).

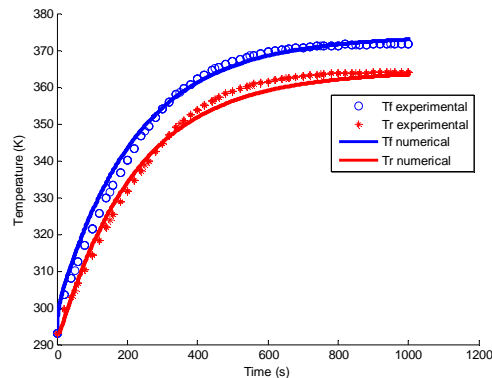


**Figure 1.** The experimental results (dots) and the numerical results (curves) with optimal thermal properties.

## Complete 2D simulation of IR heating and air convection

The IR heating apparatus was modeled in 2D for a first analysis of the air convection effect. The volume of the apparatus is represented by a rectangle, as shown in figure 2a. The small rectangle in the center of figure 2a represents the PET sheet of thickness 3 mm. The 8 IR lamps have a diameter of 4 mm. In order to simplify the study in Ansys/Fluent, they were considered as straight segments of 4 mm. It can be shown that the radiative flux is the same from a rectangle or a cylinder since the dimension of the diameter is small in regard of the distance from the sheet for example. It is the case here: the distance is 120 mm that is 30 times higher than the lamp diameter.

On these 8 lines, the IR flux is imposed to  $7900 \text{ W/m}^2$ . The other thermal boundary conditions are adiabatic and the initial temperature of the air is equal to 293 K. The calculation takes into account the radiation by solving the radiative transfer equation and the PET is assumed to be a semi-transparent medium. The radiative flux is calculated by the method of discrete ordinates which allows transforming the integro-differential radiative transfer equation into an algebraic system of equations.

Considering the velocity problem, a no-slip condition is applied at walls and at the interstices between the lamps (on the whole left, bottom and top boundaries). On the open boundary (on the right), which is the opening that allows us to follow the temperature with the thermal camera, we impose the static pressure (relative to  $P_{atm}$ )  $P_s = 0$ . The velocity is equal to zero and the air and PET temperatures are equal to 293 K at the initial condition. The continuity equation, the Navier-Stokes equation and the balance energy equation are solved to calculate the velocity, pressure and temperature fields.

It is necessary to build a hybrid mesh, structured at the boundary layers and unstructured in other volumes to limit the total number of elements. Over 250,000 cells are generated as following:

- Structured fine mesh where boundary layers develop: along the lamps, on the both sides of the PET sheet and along the top wall;
- Structured mesh between the lamps and the sheet because an upward flow of chimney type develops;
- Unstructured mesh on the region below and on the right of the sheet, in order to limit the number of computation points.

The time step is 0.005 s and the total time studied is over 400 s. The calculation is time-consuming using Fluent even for a 2D calculation. The CPU time (Pentium IV 2.99 GHz) for one simulation is about two weeks.

Figure 2b shows the results of the flow velocity at the end of 410 s. The hot lamps and the sheet also heated by the IR flux generate an increase of the air temperature near them. The temperature gradient leads to 3 vertical boundary layers along the lamps and along both sides of the PET sheet. The flow due to this local increase of temperature (chimney effect) causes a strong suction of the air flow in the bottom of the apparatus. Consequently, a cold air suction from the outside of the computational domain is observed nearly along all the open vertical boundary, except on its upper part where the air heated by the lamps and the PET sheet leaves the apparatus. A part of the entering cold flow directly goes down and leaves again the apparatus. Another part feeds the chimney between the sheet and the lamps and the boundary layer on the right of the sheet. A large recirculation zone near the top right of the sheet is surrounded by this cold flow and the hot flow coming from the chimney. One can also see that the complex flow between the lamps and the PET sheet: two air recirculation loops arise, one larger near the lamps, the other thinner near the sheet.

**Table 2.** The temperature and convection heat transfer coefficients at 410 s on the front surface

	Bottom region (y = 1 mm)	Middle region (y = 62.5 mm)	Top region (y = 125 mm)
$T (^{\circ}C)$	52	82	62
$h(\text{W/m}^2.\text{K})$	15	8	5

From the results of Fluent, one can deduce that the temperature in the sheet is strongly influenced by the air convection effect: the temperature in the bottom region is lower than elsewhere. Table 2 listed the temperature at 410 s in the bottom, middle and top of front surface of the PET sheet.

One can then calculate the heat transfer coefficient  $h$  at Prandtl number  $Pr = 0.71$  (air) from the following correlation valid for natural convection along a vertical wall heated at constant heat flux [9]:

$$h = \frac{N_u k}{y} = 0.4928 \cdot k \cdot \left( \frac{g\beta}{\nu\alpha} (T - T_\infty) \right)^{1/4} y^{-1/4} \quad (5a)$$

where  $N_u$  is the Nusselt number,  $y$  the coordinate of the vertical wall,  $g$  the gravitational acceleration,  $\beta$  the coefficient of thermal expansion,  $\alpha$  the thermal diffusivity and  $\nu$  the kinematic viscosity.

The value of  $h$  listed in table 2 can be represented as a linear function of  $y$  for sake of simplification:

$$h = h_0 - \frac{\Delta h}{L} y \quad (5b)$$

Where  $\Delta h/L = 84 \text{ W/m}^3 \cdot \text{K}$  and  $h_0 = 14 \text{ W/m}^2 \cdot \text{K}$ .

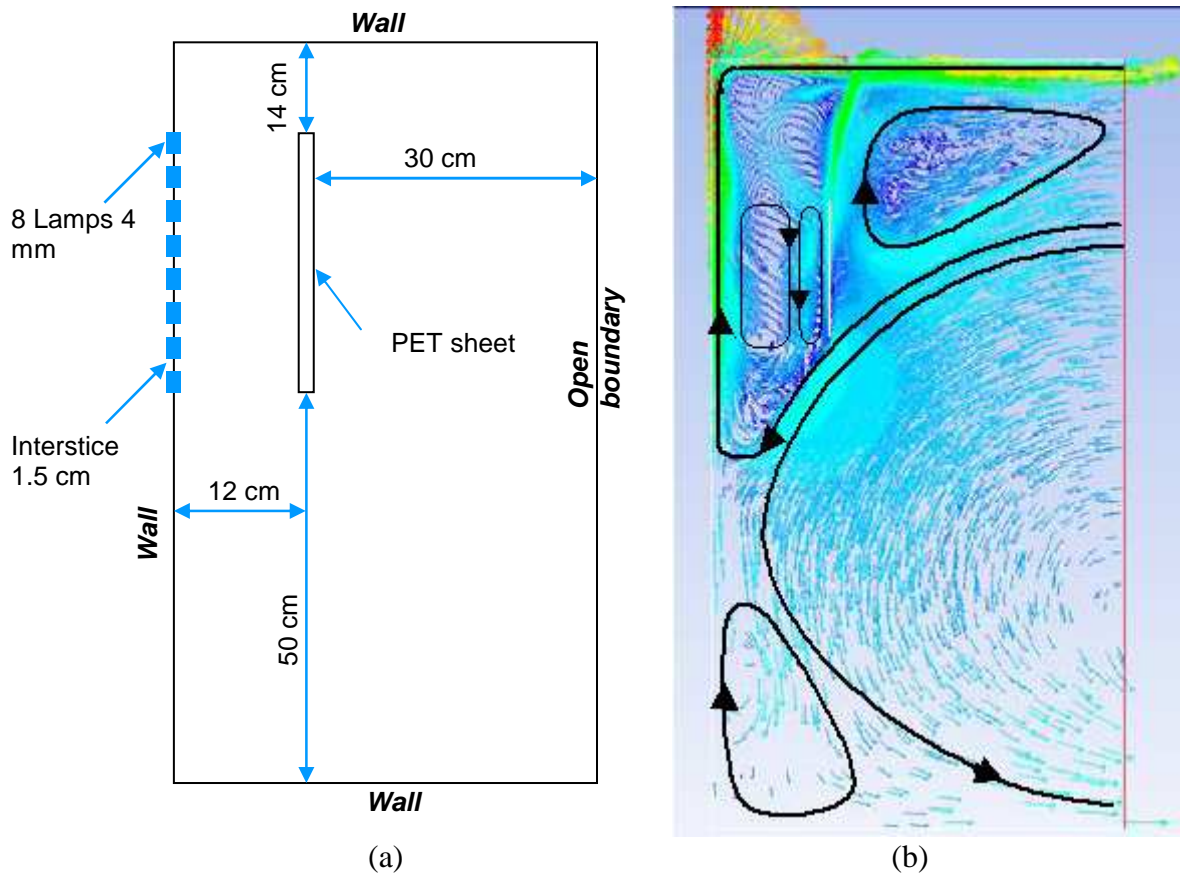


**Figure 2.** (a) Geometry of the problem; (b) Results of Ansys/Fluent at  $t=410 \text{ s}$ , air flow velocity vectors colored by the velocity magnitude

### 3D IR heating simulation with simplified approach for air convection

The complete calculation takes a lot of CPU time and is not adapted to the simulation of the IR heating of rotating preform in an industrial context. In this section, we propose to manage a 3D simulation for the PET sheet using a simplified approach for the air convection effect. The convective heat transfer coefficient  $h$  are represented in the equation 5b of the previous calculations

is introduced in the boundary conditions of the thermal problem for the PET sheet alone to mimic the air convection effect in the 3D calculation. Thanks to this simplified model for convection, using the radiative flux modelled in [7], we improve the simulation accuracy.

Figure 3 shows the comparison between the temperature of the rear surface at steady state measured by the thermal camera and the one coming from the simulation. The mean difference  $\left( \sum_{i=1}^{n=36} |\Delta T_i| / T_i \right) / n$  does not exceed 5%. This allows us to consider with confidence the calculations for more complicated geometry, such as the preform rotating in front of the lamps during the heating.

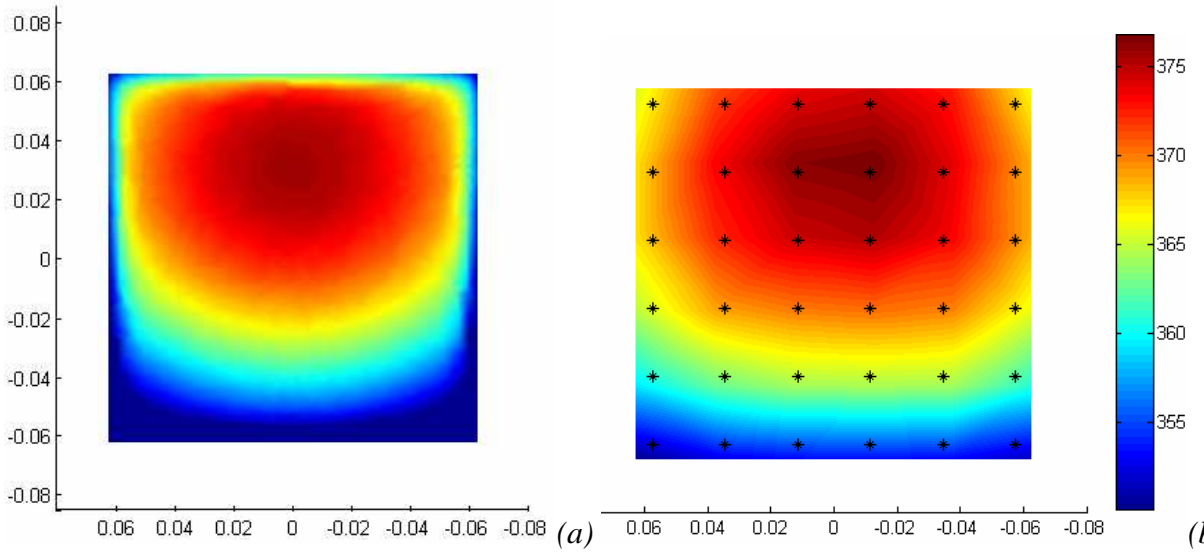


**Figure 3.** The surface temperature of the rear surface at steady state: (a) simulation results from Comsol; (b) experimental results from the thermal camera.

### The 3D IR heating simulation for PET preform

We use the same modelling based on the principle of spectral energy relation and the evaluation of the view (or form) factor in [7] to estimate the absorbed infrared radiation on PET preform. From the calculation of the intensity of the incident radiation on the cylindrical or semi-spherical part, one obtains the incident heat flux on the outer surface of the preform (figure 4). One can see that the intensity of the incident radiation reaching the outer surface of the PET preform is not uniform. At the central zone, the incident heat flux is equal to  $2500 \text{ W/m}^2$ . In the semi-spherical part, it drops quickly with the depth because of the geometry (it reaches zero at the deepest point).

The incident heat flux is calculated in Cartesian coordinates  $(x, y, z)$  and is transferred in cylindrical coordinates  $(r, \theta, z)$  (figure 4) to impose the interpolated flux in the simulation. According to the distribution and the value of the incident heat flux shown in figure 4, one chooses an exponential function for the interpolation in order to guarantee positive values of the flux for all points of the preform:

$$q_{fm} = a \exp(b\theta^2 + c\theta + dz^2 + ez + f) \quad (6)$$

where:  $a = 2.43 \text{ W/m}^2$ ,  $b = -0.86$ ,  $c = -0.0056$ ,  $d = 6.45 \text{ m}^{-2}$ ,  $e = -92.61 \text{ m}^{-1}$ ,  $f = 0.61$

From figure 4, we compare the intensity of the incident radiation calculated and the one interpolated. In the cylindrical part, the maximum difference between these two fluxes is less than 0.1%: most differences appear on the semi-spherical region.



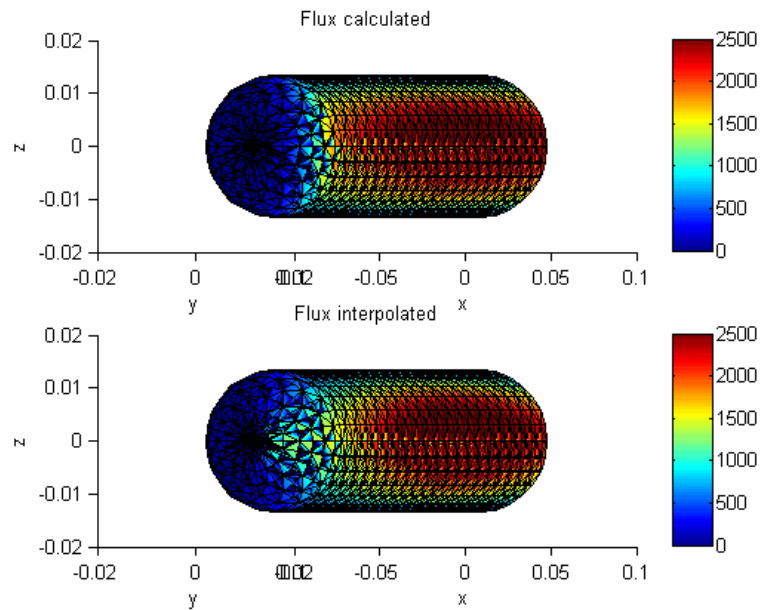


**Figure 4.** The intensity of the incident radiation on the outer surface of the preform (Visualized by Matlab): calculated (above) VS interpolated (below).

In the following, we focus on the modelling of the temperature distribution in a preform heated by IR lamps. The preform rotates at a speed of 8 rounds / minute in front of the IR lamps, generating a homogeneous heating on the loop direction of the preform. In the experimental result, 60 points on the outer surface of the preform are measured by the thermal camera to follow the evolution of the temperature. Figure 5a shows the outside temperature of the preform at quasi steady state.

To take into account the rotation of the preform, the interpolated intensity of the incident radiation of equation 6 is implemented in the simulation by software Comsol with  $\theta = \Omega t$  and  $\Omega = 8$  rounds / minute. The figure 5b shows the temperature on the outer surface of the preform at quasi steady state obtained by the numerical solution. The temperature obtained is a substantially good representation of the experimental results measured by the camera: in the center region, the difference is about 3%; in the spherical and neck parts, the difference are about 8% and 4%. In the case of a constant convective heat transfer coefficient  $h$  (without taking into account the air convection), the difference of temperature in the spherical part can reach 40%. Taking into account the air convection is of great importance.

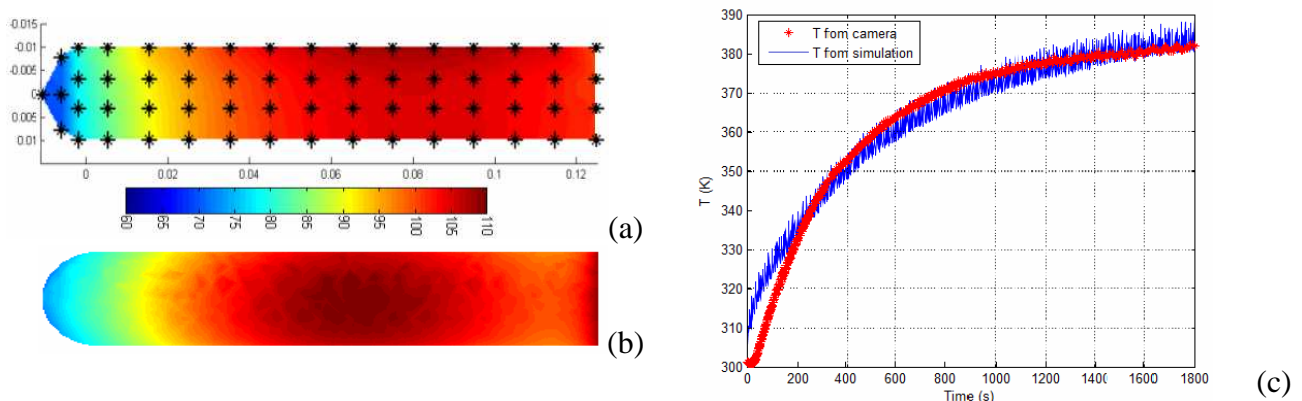


**Figure 5.** (a) Experimental results of the distribution of temperature on the outer surface of the preform at quasi steady state from thermal camera; (b) numerical results from Comsol; (c) evolution of the temperature on the center point of the outer surface

Figure 5c shows the evolution of the temperature on the center point of the outer surface obtained by simulation from Comsol and the one measured by the camera. The mean difference between the



two results is about 1%. In the simulation results, this point rotates in front of the IR lamps and that leads to oscillations in the evolution of the temperature. These oscillations can reach  $\pm 3^{\circ}\text{C}$  from the mean temperature evolution. This phenomenon does not appear on the experimental curve because the thermal camera measures the temperature always at the same location in space (i.e. the material point of the preform is not followed by the camera).

## Conclusions

Experiments have been improved (since [7,8]) to characterize the thermal properties of the PET at a temperature near or slightly above the glass transition temperature  $T_g$ . The improvement of the experimental procedure validates the identified values in regard of the classical ones in the literature.

With these identified parameters, a complete numerical simulation involving the air convection was performed in Ansys/Fluent software for the case of the PET sheet. This geometry allows considering a 2D modelling. Even with this simplification, the complete problem is time consuming. Therefore, a simplified model with the air convection effect was produced in the Comsol software to manage a 3D simulation. The convective heat transfer coefficient  $h$  obtained from the previous results of Ansys/Fluent was implemented in this simulation. There is a good agreement between the experimental and numerical solution results.

The IR heating flux coming from IR lamps was studied using radiative laws adapted to the PET preform geometry. A 3D numerical simulation with the interpolated intensity of the incident radiation was performed involving the convective heat transfer coefficient  $h$  to model the air convection effect. The conclusion is that temperature distribution on the outer surface of the preform at steady state fits well between the numerical results and the experimental results measured by the camera.

In further works, we intend to implement the temperature distribution of the preform as an initial condition to simulate accurately the ISBM process.

## References

- [1] Ph. Lebaudy, J.M. Saiter, J. Grenet, C. Vautier. Polymer, Vol 36, Iss 6, p 1217–1221, 1995.
- [2] F.M. Schmidt, Y. Le Maout, S. Monteix. J. of Materials Processing Technology, 143–144, p 225–231, 2003.
- [3] S. Monteix, F. Schmidt, Y. Le Maout. J. of Materials Processing Technology 119(1-3), p 90-97. 2001.
- [4] M. Bordival, Y. Le Maout, F.M. Schmidt. Int J Mater Form, Suppl 1:1023–1026, 2008.
- [5] F. Erchiqui, . Hamani, A. Charrette. International Journal of Thermal Sciences 48, p 73–84, 2009.
- [6] B. Cosson, F. Schmidt, Y. Le Maout, M. Bordival. Int J Mater Form, 4; 1-10, 2011.
- [7] Y.M. Luo, L. Chevalier, F. Utheza, E. Monteiro. Polymer Eng. & Science, Vol 53, Issue 12, p 2683–2695, 2013.
- [8] Y.M. Luo, L. Chevalier, F. Utheza. Proceedings of the ASME 2012 11th Biennial Conference On Engineering Systems Design And Analysis, Nantes, France, 2-4 July, 2012.
- [9] A. Bejan. Convection heat transfer, second edition. John Wiley & Sons, Inc, 1995.